AA528 Final Project
Transfer Orbit Design Proposal: Earth to Earth-Moon L4

Berit Syltebo

March 2023

1 Introduction

Equilateral libration points appear to be something out of a sci-fi movie, not a real life phenomena. However, discovery of asteroids in the Sun-Jupiter system verified the surprising theory and proved that orbits around seemingly empty space are possible if placed just right in a 3-body system. Some asteroids have even been discovered in the Earth-Moon system orbiting L4 and L5. And it turns out that these locations might have practical applications. While there may never be reason to send humans to these destinations, the possible satellite coverage from one of these orbits may be significantly useful compared to those in low Earth and geostationary orbits.

The goal of this project was to expand upon the Circular Restricted 3-Body Problem (CR3BP) discussed in this class and apply it to more complicated problems such as trajectory design. The theory behind equilateral libration points was the main point of intrigue when deciding how to best spend my time exploring the 3-body problem. In order to put together a complete analysis, proficiency in many new concepts were necessary including invariant manifold theory and machine learning techniques to optimize trajectories. Knowledge from this class could be applied when developing equations of motion and linearization for first approximations. There were definite shortfalls in my final output as much of my time was spent learning and attempting to reproduce simulations from complex models. Nevertheless, a design was proposed using a Hohmann transfer with relatively thorough

investigation of L4 dynamics upon arrival. A final orbit around L4 is realized and important design parameters such as transfer timing and velocity correction costs are considered.

2 Contributions

Two primary contributions were considered for sources of theory behind libration point stability and transfer trajectories. The first of which inspired the topic and goals for this project while the second provided a more in-depth look at the mechanics of the numerical methods and modelling.

2.1 Low-thrust transfer to the Earth-Moon triangular libration point via horseshoe orbit - Xingji He [1]

This paper analyzes the stability at the equilateral libration points to determine destination conditions for a low-thrust horseshoe orbit transfer from Earth to the chosen point - both L4 and L5 were considered. The motivation for such a transfer came from the costly nature of a direct transfer (such as Hohmann) and the approximations for these methods. Lunar gravity assists and low-thrust techniques have been explored. This paper emphasizes the use of a low-thrust system (like solar sails and ion thrusters) in tandem with utilizing a horseshoe coasting arc to minimize fuel cost.

In order to design a transfer, initial and final conditions must first be established. The paper starts by discussing the periodic orbits about L4 in order to realize potential insertion points. These periodic orbits consist of short and long period options which can be scaled using the same fundamental frequencies. One orbit distance is considered to compare the linear approximation with the nonlinear. More cases are discussed in the next contribution and to what extent the linear approximation is sufficient.

For the transfer, the contributors noted the similarities between the natural horseshoe orbit and realized low-thrust trajectory from Earth to L4. This idea provides the foundation for the purpose of this paper: utilize the natural horseshoe orbit as a coasting arc for for the low-thrust trajectory. As a result, three phases were introduced for the complete trajectory: get from Earth to the horseshoe coasting arc, travel along the coasting for some amount of time, and get from the coasting arc to the predetermined insertion

point about L4. A visual of the concept of operations as described above can be found in Figure 1.

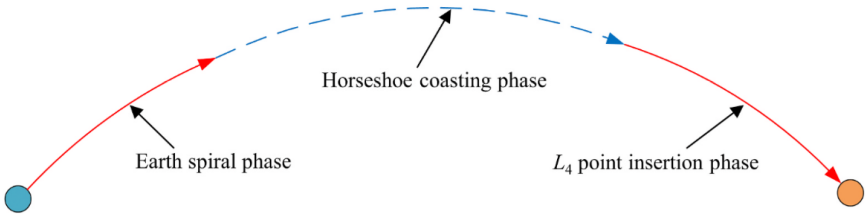

Figure 1: Earth to L4 transfer trajectory concept of operations

Eight possibilities were explored with varying thrust magnitudes. Four of these possibilities are shared in this paper and can be found in Figure 2. There are obvious pros and cons to this method that can be seen right off the bat; the most obvious is the total transit time. Taking a direct transfer would take less than a week to arrive at L4 while this low-thrust method would take on the order of years. The option with the smallest transfer time - not included in this report - was still 269 days. Despite the stark difference in time, missions of this type likely will not be time sensitive. For modern day purposes, visiting the equilateral libration points would be investigative or for satellite placement and therefore would not need to be manned. This idea could work well for a non-urgent mission with a payload of only instrumentation.

A major pro of this method is the minimal and optimized fuel consumption. It is well established that low-thrust propulsion options - namely ion thrusters - typically have superior efficiency against their chemical propulsion counterparts. This contribution computed the fuel fraction (mass of propellant over total mass of spacecraft) to be an average of 3% across all eight cases with case B being the most effective at 1.54%.

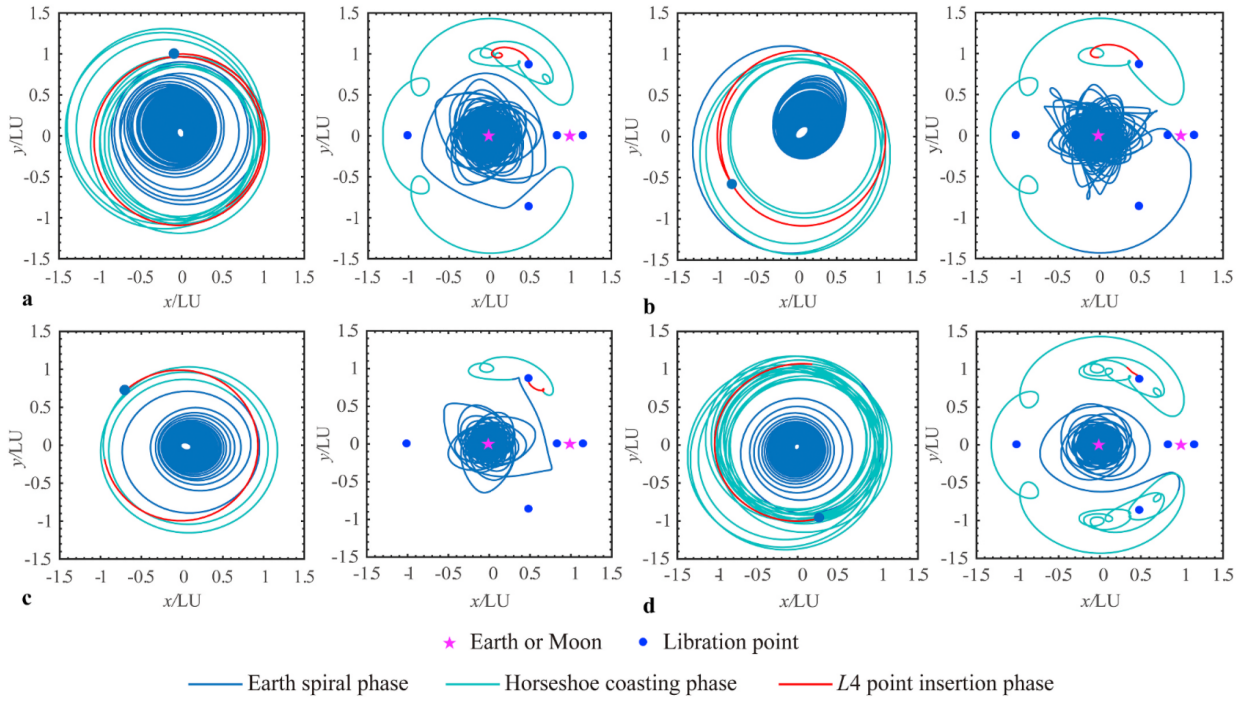

No.	Thrust (mN)	Insertion point	Deorbit point	E-H transfer time (day)	Coasting time (day)	H-L_4 transfer time (day)	Total transfer time (day)	Apogee of parking orbit (km)
A	10	0.415	0.600	1147	235	40	1422	32335
B	10	0.450	0.400	794	139	35	968	61118
C	30	0.630	0.325	353	9	26	388	39058
D	30	0.100	0.700	470	459	16	945	18706

Figure 2: Four potential transfer trajectories in the Earth-centered inertial frame (left) and barycentric synodic frame (right), and their associated numeric properties

2.2 Investigation of transfer trajectories to and from the equilateral libration points L4 and L5 in the Earth-Moon system - Lucia R. Irrgang [2]

The motivation of this contribution was to utilize the advantageous location of the equilateral libration points for applications like deep-space communication by placing a satellite at one of these points. The paper bases its analysis around the Circular Restricted 3-Body Problem (CR3BP) and thus discusses

the relevant dynamics from this approach (Section 2); this includes equilibrium points, linearization techniques, periodic solutions for libration point orbits, and invariant manifold theory. Some of these numerical methods and dynamics will be discussed more in-depth in the next section.

The third section of this paper explores motion about the equilateral libration points to determine periodic orbits using accurate models. The limitations of linear approximations for these orbits are thoroughly investigated to determine to what extent this simplified model is effective. This analysis is conducted for both short and long period orbits. It is clear from Figure 3 that the linear approximation breaks down as orbit trajectory gets further and further away from the libration point.

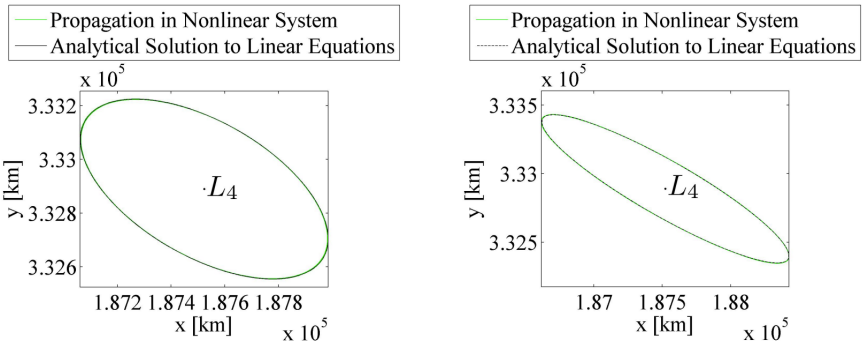

(a) Insertion distance ≈ 384km

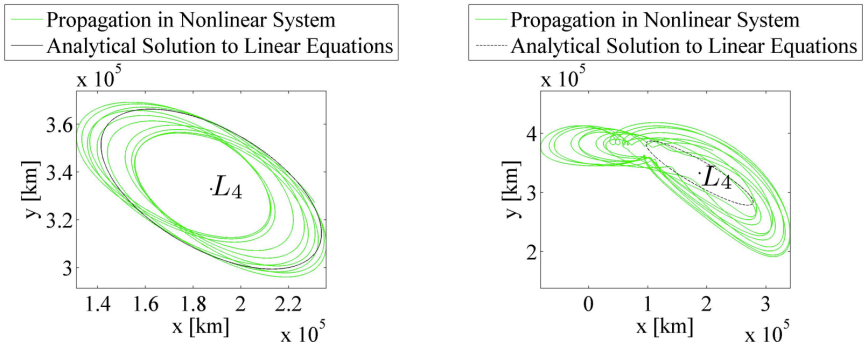

(b) Insertion distance ≈ 38400km

Figure 3: Comparison of linear and non-linear modelling for short and long period orbits about L4 with varying insertion distances

Due to the inaccuracies of linear approximations about these libration

points, proceeding analyses only use nonlinear models. This allows for much more variability in periodic orbit size to suite a wider range of mission specifications. In fact, the short period orbit chosen as the final destination for the transfer is quite large in relation to the limitations of linearization so the increase in robustness was essential.

Rather than starting at Earth, the paper focuses on transfer to and from an L2 periodic orbit using the stable and unstable manifolds as ideal trajectories for the spacecraft. Section 4 covers planar transfers while Section 5 covers 3-dimensional. For the sake of this project, only planar will be summarized and considered. The derivation process highlighted was for a transfer from L4 to L2 following a stable manifold but also briefly explored how to get to L4 or L5 from L2 from an unstable manifold. An example of this trajectory can be found in Figure 4 where the magenta line represents the transfer starting at the magenta star. The transfer makes almost a full revolution about L2 before showing a significant difference between the periodic orbit and the transfer.

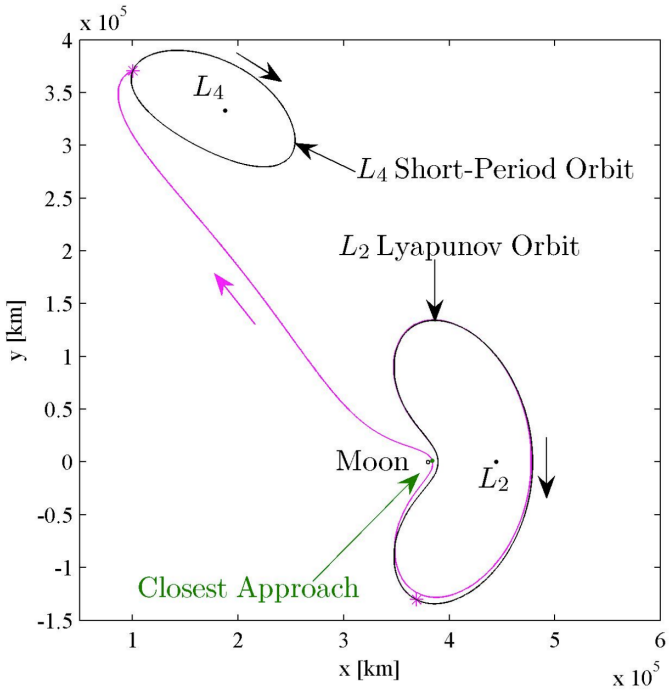

Figure 4: Example trajectory from L2 to L4 orbit

3 Theory & Analysis Techniques

The theory discussed in this section all comes from the contribution discussed in Section 2.2. While a lot of the same techniques are used in the first contribution, there was no thorough explanation as to how each method was applied. That being said, the topics explained here are relevant to both papers. It is also important to note that the topic of invariant manifolds has been omitted due to complexity that deserved more time to explain than the time limitations on this project permitted.

3.1 Circular Restricted 3-Body Problem

The circular restricted 3-body problem is constructed to better model 3-body systems with two dominant masses, one typically being much larger than the other. The Earth-Moon system is an obvious example of this as lunar gravitation has a non-negligible effect on bodies in the vicinity of Earth. Thus the 2-body problem loses it's effectiveness. Equation 1 shows how Newton's Law of Gravitation can be extended to an n-body problem.

$$\vec{F}_i = \tilde{G} \sum_{j=1, j\neq i}^{n} \frac{m_i m_j}{r_{ji}^3} \vec{r}_{ji} \tag{1}$$

The equations of motion in the rotating frame for a body travelling in a system with two dominant masses can be modelled using Equation 2. The necessary quantities to complete these expressions are shown below where μ is the mass ratio, $\vec{d}$ is the distance from m_1 (Earth), and $\vec{r}$ is the distance from m_2 (Moon).

$$\mu = \frac{m_2}{m_1 + m_2}$$

$$\vec{d} = (x + \mu)\hat{x} + (y)\hat{y} + (z)\hat{z}$$

$$\vec{r} = (x - 1 + \mu)\hat{x} + (y)\hat{y} + (z)\hat{z}$$

$$\begin{aligned}
\ddot{x} - 2\dot{y} - x &= -\frac{(1-\mu)(x+\mu)}{d^3} - \frac{\mu(x-1+\mu)}{r^3} \\
\ddot{y} + 2\dot{x} - y &= -\frac{(1-\mu)y}{d^3} - \frac{\mu y}{r^3} \\
\ddot{z} &= -\frac{(1-\mu)z}{d^3} - \frac{\mu z}{r^3}
\end{aligned} \tag{2}$$

The potential energy of this body, which I will now refer to as the spacecraft, can then be computed using Equation 3.

$$U = \frac{1}{2}(x^2 + y^2) + \frac{(1-\mu)}{d} + \frac{\mu}{r} \tag{3}$$

Solving for the potential energy has very useful applications such as finding the Jacobi Constant; this can be computed using Equation 4. This constant reveals zero-velocity surfaces and contours (ZVS and ZVC) which can be used to determine where a body can go with its current energy state. To put it simply, this value dictates zones for which a body can and can't enter. Intuitively, if a body does not have enough energy to enter a high energy state, it is impossible to do so. For example, if a rocket does not have enough energy to reach the Karman line, it will never get to space.

$$C = 2U - (\dot{x}^2 + \dot{y}^2 + \dot{z}^2) \tag{4}$$

3.2 Libration Point Dynamics Linearization

To simplify the derivation of orbits about the libration points - specifically L4 - the rotating frame can be shifted such that the origin is located at L4. The transformation between these frames can be found in Equation 5 where ξ, η, and ζ make up the spacecraft's distance from L4 in the x, y, and z directions, respectively.

$$\begin{aligned}
x &= x_{L_i} + \xi \\
y &= y_{L_i} + \eta \\
z &= z_{L_i} + \zeta
\end{aligned} \tag{5}$$

It turns out that the second order partials of the potential energy equation make up a set of useful quantities. Using the notation that $U_{ab} = \frac{\delta^2 U}{\delta a \delta b}$, these partials are computed in Equation 6.

$$
\begin{aligned}
U_{xx} &= 1 - \frac{(1-\mu)}{d^3} - \frac{\mu}{r^3} + \frac{3(1-\mu)(x+\mu)^2}{d^5} + \frac{3\mu(x-1+\mu)^2}{r^5} \\
U_{xy} &= \frac{3(1-\mu)(x+\mu)y}{d^5} + \frac{3\mu(x-1+\mu)y}{r^5} = U_{yx} \\
U_{xz} &= \frac{3(1-\mu)(x+\mu)z}{d^5} + \frac{3\mu(x-1+\mu)z}{r^5} = U_{zx} \\
U_{yy} &= 1 - \frac{(1-\mu)}{d^3} - \frac{\mu}{r^3} + \frac{3(1-\mu)y^2}{d^5} + \frac{3\mu y^2}{r^5} \\
U_{yz} &= \frac{3(1-\mu)yz}{d^5} + \frac{3}{r^5} = U_{zy} \\
U_{zz} &= -\frac{(1-\mu)}{d^3} - \frac{\mu}{r^3} + \frac{3(1-\mu)z^2}{d^5} + \frac{3\mu z^2}{r^5}
\end{aligned} \tag{6}
$$

The new equations of motion for the spacecraft about a libration point are shown in Equation 7 where $U_{ab}|_{\vec{X}_{L_i}}$ is the specified partial evaluated at the relevant libration point.

$$
\begin{aligned}
\ddot{\xi} + 2\dot{\eta} &= U_{xx}|_{\vec{X}_{L_i}}\xi + U_{xy}|_{\vec{X}_{L_i}}\eta \\
\ddot{\eta} + 2\dot{\xi} &= U_{yx}|_{\vec{X}_{L_i}}\xi + U_{yy}|_{\vec{X}_{L_i}}\eta \\
\ddot{\zeta} &= U_{zz}|_{\vec{X}_{L_i}}\zeta
\end{aligned} \tag{7}
$$

The in-plane frequencies can then be found using the characteristic polynomial in Equation 8. These are useful in determining the necessary states to maintain a simple periodic orbit about the given libration point.

$$
\lambda^4 + \left(4 - U_{xx}|_{\vec{X}_{L_i}} - U_{yy}|_{\vec{X}_{L_i}}\right)\lambda^2 + U_{xx}|_{\vec{X}_{L_i}}U_{yy}|_{\vec{X}_{L_i}} - U_{xy}|^2_{\vec{X}_{L_i}} = 0 \tag{8}
$$

3.2.1 L4 & L5 Linearization

Evaluating Equation 6 at the equilateral libration points yield the associated potential energy partials. The surprising simplification of these constants come from the geometric location of these libration points where, in non-dimensional units, they are located at $\left(\frac{1}{2} - \mu, \pm\frac{\sqrt{3}}{2}\right)$ with the positive y coordinate corresponding to L4.

$$
\begin{aligned}
U_{xx}|_{\vec{X}_{L_{4,5}}} &= \frac{3}{4} \\
U_{yy}|_{\vec{X}_{L_{4,5}}} &= \frac{9}{4} \\
U_{xy}|_{\vec{X}_{L_4}} &= \frac{3\sqrt{3}}{2}\left(\mu - \frac{1}{2}\right) \\
U_{xy}|_{\vec{X}_{L_5}} &= -\frac{3\sqrt{3}}{2}\left(\mu - \frac{1}{2}\right) \\
U_{zz}|_{\vec{X}_{L_{4,5}}} &= -1
\end{aligned}
\tag{9}
$$

The solution to Equation 8 at the equilateral points can be found in Equation 10 where the in-plane frequencies are purely dependent upon the mass ratio, μ. Proceeding this expression reveal the derivation of constants s_1 and s_2 which define the magnitude of these in-plane frequencies and are used to compute the long and short period orbits, respectively.

$$
\begin{aligned}
\lambda_{1,2} &= \pm\sqrt{\frac{-1 + \sqrt{1 - 27\mu + 27\mu^2}}{2}} \\
\lambda_{3,4} &= \pm\sqrt{\frac{-1 - \sqrt{1 - 27\mu + 27\mu^2}}{2}}
\end{aligned}
\tag{10}
$$

$$
\lambda_{1,2} = \pm s_1 i \qquad \lambda_{3,4} = \pm s_2 i
$$

The constants Γ_1 and Γ_2 are then used to obtain the initial velocity components in the xy-plane as seen in Equation 12. Of course, the initial position must first be chosen to obtain these conditions, or vice versa, to acquire a complete initial state for the dynamical system.

$$
\begin{aligned}
\Gamma_1 &= \left(\frac{s_1^2 + U_{xx}|_{\vec{X}_{L_i}}}{4s_1^2 + U_{xy}|_{\vec{X}_{L_i}}}\right)^2 \\
\Gamma_2 &= \left(\frac{s_2^2 + U_{xx}|_{\vec{X}_{L_i}}}{4s_2^2 + U_{xy}|_{\vec{X}_{L_i}}}\right)^2
\end{aligned}
\tag{11}
$$

$$\begin{aligned}\dot{\xi}_0 &= \frac{1}{2}\left(U_{xy}|_{\vec{X}_{L_i}}\xi_0 + \frac{\eta_0}{\Gamma_i}\right)\\ \dot{\eta}_0 &= -\frac{1}{2}\left(\left(s_i^2 + U_{xx}|_{\vec{X}_{L_i}}\right)\xi_0 + U_{xy}|_{\vec{X}_{L_i}}\eta_0\right)\end{aligned} \tag{12}$$

With the initial state fully realized, the 2-dimensional motion can be modelled using Equation 13 which is in non-dimensional time, τ.

$$\begin{aligned}\xi &= \xi_0\cos(s_i\tau) + \frac{\dot{\xi}_0}{s_i}\sin(s_i\tau)\\ \eta &= \eta_0\cos(s_i\tau) + \frac{\dot{\eta}_0}{s_i}\sin(s_i\tau)\end{aligned} \tag{13}$$

3.3 Multiple Shooting Method

The premise of the multiple shooting method is to solve for initial conditions, compare against a nominal path, compute the error, correct the error, and iterate until the error is negligible. The first step is to define the error which requires a reference as an ideal solution. We can define the nominal trajectory with the following state, $\vec{x}_n(\tau)$:

$$\vec{x}_n(\tau) = \begin{bmatrix} x_n(\tau) & y_n(\tau) & z_n(\tau) & \dot{x}_n(\tau) & \dot{y}_n(\tau) & \dot{z}_n(\tau)\end{bmatrix}^T$$

The difference from the nominal solution as a function of time, τ, can then be defined by $\delta\vec{x}(\tau)$ shown in Equation 15.

$$\delta\vec{x}(\tau) = \vec{x}(\tau) - \vec{x}_n(\tau) \tag{14}$$

The state space for the deviation from nominal state is then defined in Equation 15 with $A(\tau)$ being the state transition matrix defined in Equation 16. For this matrix, the potential energy partials are evaluated at the nominal solution; while the derivation of this matrix is not included in this paper, it is fairly simple to obtain when the equations of motion are written in terms of the potential energy at a given state.

$$\delta\dot{\vec{x}}(\tau) = A(\tau)\delta\vec{x}(\tau) \tag{15}$$

$$A(\tau) = \begin{bmatrix} 0 & 0 & 0 & 1 & 0 & 0 \\ 0 & 0 & 0 & 0 & 1 & 0 \\ 0 & 0 & 0 & 0 & 0 & 1 \\ U_{xx}|_{\vec{x}_n(\tau)} & U_{xy}|_{\vec{x}_n(\tau)} & U_{xz}|_{\vec{x}_n(\tau)} & 0 & 2 & 0 \\ U_{yx}|_{\vec{x}_n(\tau)} & U_{yy}|_{\vec{x}_n(\tau)} & U_{yz}|_{\vec{x}_n(\tau)} & -2 & 0 & 0 \\ U_{zx}|_{\vec{x}_n(\tau)} & U_{zy}|_{\vec{x}_n(\tau)} & U_{zz}|_{\vec{x}_n(\tau)} & 0 & 0 & 0 \end{bmatrix} \tag{16}$$

The relationship between one state at some initial time, τ_0, and some later time, τ, is then defined by the 6×6 matrix, $\Phi(\tau, \tau_0)$, in Equation 17. It's relationship with the state transition matrix then becomes the differential equation in Equation 18.

$$\Phi(\tau, \tau_0) = \frac{\delta\vec{x}(\tau)}{\delta\vec{x}(\tau_0)} \tag{17}$$

$$\dot{\Phi}(\tau, \tau_0) = A(\tau)\Phi(\tau, \tau_0) \tag{18}$$

The properties described above are useful when there is some desired state for some time, τ_f, often described as the final state. If the magnitude of τ_f is a design constraint, Equation 19 is useful in determining an initial state following this constraint, and converging to the nominal solution where the final state is known.

$$\delta\vec{x}(\tau_f) = \begin{bmatrix} \Phi(\tau_f, \tau_0) & \dot{\vec{x}}(\tau_f) \end{bmatrix} \begin{bmatrix} \delta\vec{x}(\tau_0) \\ \delta\tau_f \end{bmatrix} \tag{19}$$

In this problem, the final velocity is not a constraint on the trajectory design; when an L4 periodic orbit is reached, some Δv correction can be used to properly proceed to the next phase of the mission. Moreover, initial position may be known such that the only condition of interest to solve for a possible trajectory is the initial velocity. As such, we can define the error as the negative distance of the spacecraft from the final desired position where this deviation is defined below as $\delta\vec{r}(\tau)$. Evaluated at τ_f, error $\vec{e}$ is obtained per Equation 20.

$$\delta\vec{r}(\tau) = \begin{bmatrix} \delta x(\tau) & \delta y(\tau) & \delta z(\tau) \end{bmatrix}^T$$

$$\vec{e} = -\delta\vec{r}(\tau_f) \tag{20}$$

Based on this output error, a correction to the initial velocity guess is made via Equation 21. It is important to note that the 3×3 transition matrix in this expression comes directly from $\Phi(\tau, \tau_0)$ evaluated at τ_f; one can take the first three rows and last three columns of $\Phi(\tau_f, \tau_0)$. If τ_f is not known this process can also find the time required to reach the final state.

$$\begin{bmatrix} \delta\vec{v}(\tau_0) \\ \delta\tau_f \end{bmatrix} = \begin{bmatrix} \frac{\delta x(\tau_f)}{\delta \dot{x}(\tau_0)} & \frac{\delta x(\tau_f)}{\delta \dot{y}(\tau_0)} & \frac{\delta x(\tau_f)}{\delta \dot{z}(\tau_0)} & \dot{x}(\tau_f) \\ \frac{\delta y(\tau_f)}{\delta \dot{x}(\tau_0)} & \frac{\delta y(\tau_f)}{\delta \dot{y}(\tau_0)} & \frac{\delta y(\tau_f)}{\delta \dot{z}(\tau_0)} & \dot{y}(\tau_f) \\ \frac{\delta z(\tau_f)}{\delta \dot{x}(\tau_0)} & \frac{\delta z(\tau_f)}{\delta \dot{y}(\tau_0)} & \frac{\delta z(\tau_f)}{\delta \dot{z}(\tau_0)} & \dot{z}(\tau_f) \end{bmatrix}^+ \vec{e} \tag{21}$$

This method is iterated until the error vector is sufficiently small such that the initial velocity gets the spacecraft to the desired final state, $\vec{x}_n(\tau_f)$, with some defined tolerable deviation.

4 Verification of Contribution Work

4.1 L4 Periodic Orbits

Knowing that rough initial and final conditions are necessary before starting a transfer trajectory design, I started by reproducing the motion about L4 using a linear approximation. Section 3.2.1 reveals the derivation for these dynamics such that only the mass ratio, μ, is need to create a skeleton for the equations of motion. The in-plane frequencies are easily computed using Equation 8 such that s_1 and s_2 are found. These computed quantities are shown below:

$$s_1 = 0.29820789544347032$$

$$s_2 = 0.95450094347526815$$

The paper by Lucia R. Irrgang is somewhat misleading in it's derivation of the initial conditions to complete Equation 13. I attempted to use the suggested initial conditions for both long and short period orbits but wasn't able to recreate the results. I later realized that the initial conditions given were in dimensional units and Equation 13 needed velocity components in terms of non-dimensional time. Using the provided equations to derive the velocity from scratch, I obtained wildly different numbers from those provided but ended up matching the results in the paper. The table below shows

the proper inputs for the equations of motion and how the velocity vector compares in dimensional units.

s_i	s_2 (short period)	s_1 (long period)
ξ_0 (km)	384.388174	384.388174
$\dot{\xi}_0$	243.59871675129397	243.59871675129397
$\dot{\eta}_0$	-319.2482263014549	-161.2369911985452
$\dot{\xi}_0$ (km/s)	$6.493012243087153\times10^{-4}$	$6.493012243087153\times10^{-4}$
$\dot{\eta}_0$ (km/s)	$-8.509362006775028\times10^{-4}$	$-4.297671260030953\times10^{-4}$

To simplify the computation of these periodic orbits, the initial position was chosen with a y-position equal to that of L4 (ie. $\eta_0 = 0$). The result is equivalent ξ_0 properties between the short and long period orbits. Variations in the initial condition properties only appear in $\dot{\eta}_0$. Also important to note is the precision in these measurements; while L4 is marginally stable, these orbits behave such that any perturbations will cause the spacecraft to follow a new orbit and not converge back to the original. To maintain a stable orbit, a control system would need to be implemented to either make continuous or periodic corrections.

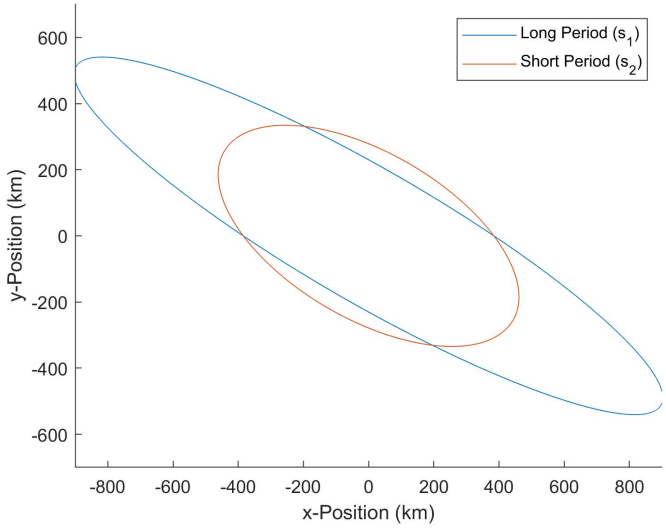

Figure 5: Simulation of short and long period orbits about L4 with an initial position of (384.388174,0)

Implementation of the equations of motion with the computed initial conditions can be found in Figure 5.

4.2 L4 Zero-Velocity Surface

Using Equations 3 and 4 to obtain the Jacobi Constant associated with L4, the Zero-Velocity Surface (ZVS) was plotted as shown in Figure 6. In a previous assignment, the ZVS was also computed for L2 which can be found in Figure 7.

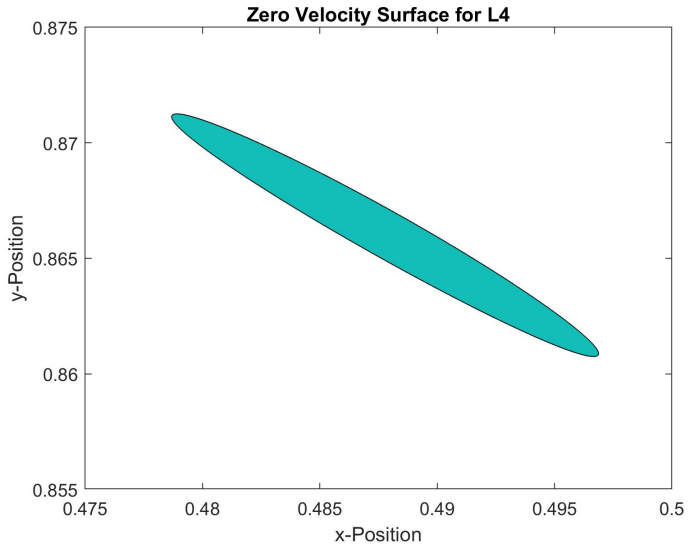

Figure 6: Zero Velocity Surface for L4 in non-dimensional units centered in the rotating frame

The purpose for studying these ZVS's is to determine what energy a spacecraft would need to get to L4. Studying the invariant manifolds associated with L2, one can choose a path which passes closest to L4; none of which will ever penetrate the L4 ZVS. Once this path is selected, a transfer from the manifold to L4 can be selected using the multiple shooting method. Due to the complexity of this process and deep understanding of multiple complicated ideas, I was unable to continue this road of analysis. For the sake of time and my own sanity, I chose to give up on modelling these manifolds and implementing the multiple shooting method.

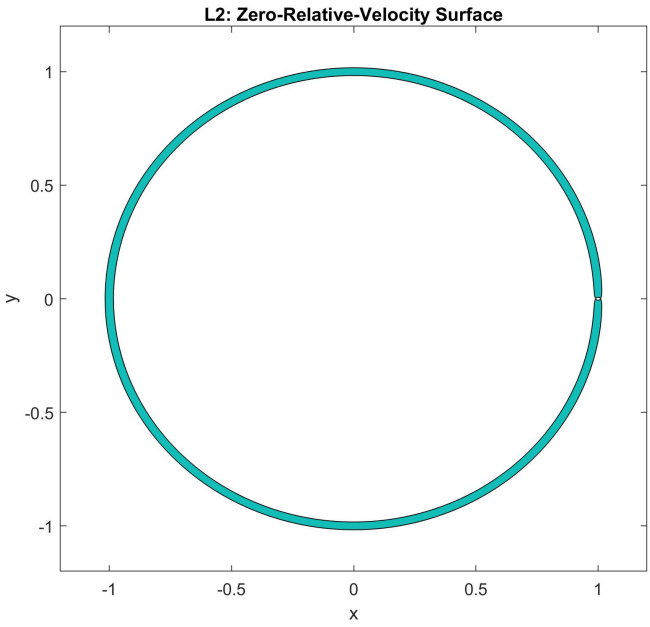

Figure 7: Zero Velocity Surface for L2 in non-dimensional units centered in the rotating frame

4.3 Hohmann Transfer Design

Since I promised to provide a transfer trajectory from Earth to L4, I used the rest of my limited time (much was lost to attempts at the multiple shooting method) designing a Hohmann transfer using my results from Section 4.1.

Before designing the transfer properties, it's important to take into account the assumptions that come with a 2-body solution. A very simple model of the 3-body problem is using the method of patched conics which stitches together a series of 2-body problems. The thresholds between these 'patches' are defined by the sphere of influences of the dominant bodies in the system. When a spacecraft enters a new sphere of influence, the dynamics can then be modelled using purely using the gravitation of that body.

A comparison of the Sphere of Influence (SOI) of the Moon with that of the Earth can be found in Figure 8. Due to the mass difference between these bodies, the Moon's SOI is clearly much smaller than the Earth's. In fact, the Moon's is completed encompassed by the Earth's. Thus, to apply the method

of patched conics, the dynamics of a spacecraft can be approximated using the Moon's gravity alone if it falls within $SOI_{☾}$, and the Earth's gravitation if it doesn't. This produces a crude model but can be used as a good first approximation in a design process.

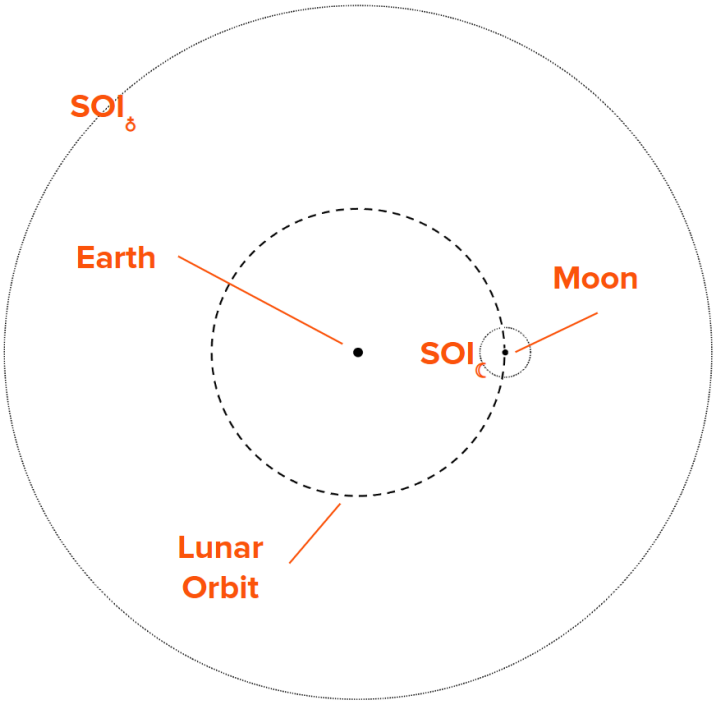

Figure 8: Scale drawing the Sphere of Influence comparison betweem Moon and Earth

Assuming the lunar orbit is circular, an elliptical orbit from Earth to L4 orbit can be easily computed. Low Earth Orbit (LEO) at 300km altitude was chosen as the starting position for the spacecraft to simplify computation. The resulting properties of the orbit shape are summarized below:

$$e = 0.9657$$

$$a = 194685 \text{ km}$$

$$T_{transfer} = 4.947 \text{ days}$$

Next, using the transfer time, the time of transfer initiation was determined. The Moon travels 65.192° during the transfer and knowing that L4 is 60° ahead of the Moon, the fist burn (from LEO to transfer) would need to occur when the Moon is 125.192° behind the projected apogee. This is reflected in the transfer orbit simulation found in Figure 9 which is depicted in the Earth-Centered Inertial frame (ECI).

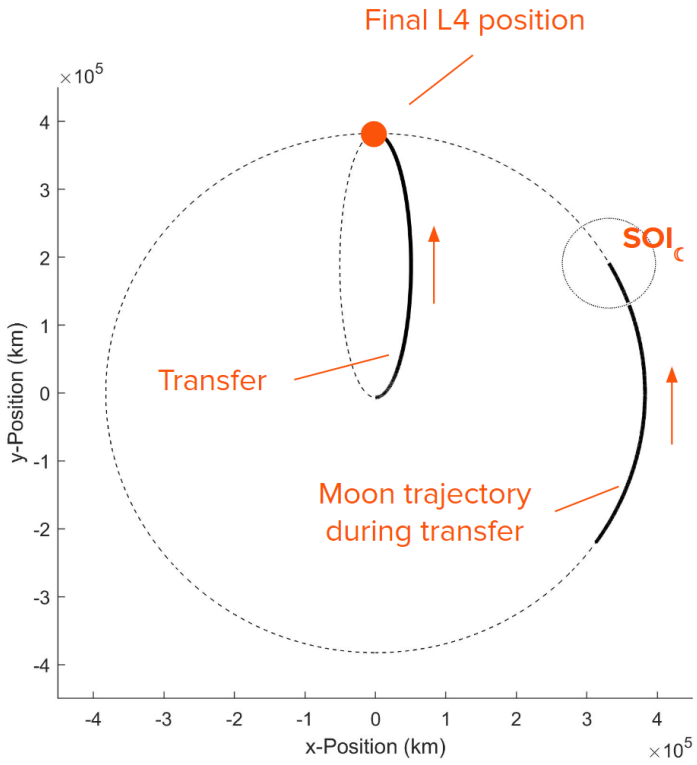

Figure 9: ECI transfer trajectory simulation including moon path and SOI

It is clear based on the to-scale drawing above that the transfer never falls within the sphere of influence of the moon and thus the dynamics of the spacecraft can be modelled using Earth's gravitation alone based on the rules of patched conics.

The last step I took in my analysis was solving for the necessary velocity corrections associated with the chosen transfer. Since the correction to get into the L4 periodic orbit are so small, they were not considered in my

analysis. However, due to sensitivity around these points, these corrections would not be negligible for a real mission. A summary of these calculations are found below:

$$\begin{aligned} v_{\text{LEO}} &= 7.726\text{km/s} \\ v_{\text{transfer,p}} &= 10.832\text{km/s} \\ \Delta v_1 &= 3.106\text{km/s} \end{aligned}$$

$$\begin{aligned} v_{\text{transfer,a}} &= 0.189\text{km/s} \\ v_{\leftmoon} &= 1.021\text{km/s} \\ \Delta v_2 &= 0.832\text{km/s} \end{aligned}$$

5 Contribution Assessment

The contribution discussed in Section 2.1 was very intriguing and prompted the topic of this project. However, I spent a day trying to make sense of the methods used and got nowhere. The vagueness in description of approach became very frustrating and with my current knowledge, I wouldn't have been able to replicate any of the work. Also, in the final section of the paper, the team explored fuel consumption and cost for each of their transfer options. It seemed unreasonable to only start considering consumption once the spacecraft reached the energy of L1. The whole purpose of this study was to show the pros of a low-thrust transfer over other methods like direct transfer and neglected an imperative section of the trajectory: the spiral away from Earth. I would have liked to see a more in-depth look at how much fuel and resources are truly conserved using this method over competitive studies and a Hohmann transfer.

The second paper - discussed in Section 2.2 - gives a much more in-depth mathematical background for similar applications. This is how I was able to obtain models for the periodic orbits around L4. The only issue I had with it was how their transfer trajectory was from L2 to L4 rather than Earth to L4 as the title implied. There seemed to be a lot more investigation of the L2 manifolds and halo orbits than how to get to and from the equilateral libration points in practical scenarios. There was no explanation (that I could find) for why they were only considering transit with one collinear point and what real life purpose that would serve. I think the multiple shooting method

could still be used with an Earth to L4 transfer and would like to see out how that would work. Perhaps the research turned into something the author wasn't expecting and deviated from their initial motivations.

6 Conclusion

This was a very enlightening project and if I had more time or more reason than curiosity to continue, there are plenty of concepts I would like to investigate further. The biggest problem I'd want to tackle would be constructing a working algorithm using the multiple shooting method to obtain a transfer from Earth to L4. As discussed in this paper, the Hohmann transfer is not a resource-efficient way to get anymore and missions to the equilateral libration points likely wouldn't be time-sensitive, allowing for more energy efficient propulsion methods and trajectories. Moreover, I think this is a cool example of machine learning in aerospace and would like to become more proficient in optimization.

If I were start over, I would choose to only focus on a periodic orbit around L4 and design a control system to keep a spacecraft orbiting in a desired trajectory. It would have been nice to apply my controls knowledge outside of stability to this problem and I didn't leave myself enough room to do so. For the time period given for this project, I was definitely too ambitious and ended up doing a lot more learning than applying. But this wasn't necessarily a bad thing; I enjoyed learning about how the physics of the universe can be modelled and think I gained a lot. I am proud of the work I was able to produce despite the Hohmann transfer being unsatisfying to my standards. I hope to find time to learn more about invariant manifolds and the multiple shooting method.

References

[1] He, X., Liang, Y., Xu, M., amp; Zheng, Y. (2020). Low-thrust transfer to the Earth-moon triangular libration point via Horseshoe Orbit. Acta Astronautica, 177, 111–121. https://doi.org/10.1016/j.actaastro.2020.07.014

[2] Irrgang, L. R. (2008). Investigation Of Transfer Trajectories To And From The Equilateral Libration Points L4 And L5 In The Earth-Moon System (thesis).